HUMAN GENE THERAPY 22:865–871 (July 2011)

DOI: 10.1089/hum.2010.199

Brief Reports

Characterization of a Transgenic Short Hairpin RNA-Induced Murine Model of Tafazzin Deficiency

Meghan S. Soustek,[1,2] Darin J. Falk,[1,2] Cathryn S. Mah,[1,2] Matthew J. Toth,[3] Michael Schlame,[3,4] Alfred S. Lewin,[5] and Barry J. Byrne[1,2,3,5]

Abstract

Barth's syndrome (BTHS) is an X-linked mitochondrial disease that is due to a mutation in the *Tafazzin* (*TAZ*) gene. Based on sequence homology, TAZ has been characterized as an acyltransferase involved in the metabolism of cardiolipin (CL), a unique phospholipid almost exclusively located in the mitochondrial inner membrane. Yeast, *Drosophila*, and zebrafish models have been invaluable in elucidating the role of TAZ in BTHS, but until recently a mammalian model to study the disease has been lacking. Based on *in vitro* evidence of RNA-mediated TAZ depletion, an inducible short hairpin RNA (shRNA)-mediated TAZ knockdown (TAZKD) mouse model has been developed (TaconicArtemis GmbH, Cologne, Germany), and herein we describe the assessment of this mouse line as a model of BTHS. Upon induction of the TAZ-specific shRNA *in vivo*, transgenic mouse TAZ mRNA levels were reduced by >89% in cardiac and skeletal muscle. TAZ deficiency led to the absence of tetralineoyl-CL and accumulation of monolyso-CL in cardiac muscle. Furthermore, mitochondrial morphology from cardiac and skeletal muscle was altered. Skeletal muscle mitochondria demonstrated disrupted cristae, and cardiac mitochondria were significantly enlarged and displace neighboring myofibrils. Physiological measurements demonstrated a reduction in isometric contractile strength of the soleus and a reduction in cardiac left ventricular ejection fraction of TAZKD mice compared with control animals. Therefore, the inducible TAZ-deficient model exhibits some of the molecular and clinical characteristics of BTHS patients and may ultimately help to improve our understanding of BTHS-related cardioskeletal myopathy as well as serve as an important tool in developing therapeutic strategies for BTHS.

Introduction

Barth's syndrome (BTHS) is an X-linked mitochondrial disease that has been associated with loss-of-function mutations in the *Tafazzin* (*TAZ*) gene located at the distal portion of Xq28 (Barth *et al*., 1983; Bolhuis *et al*., 1991; Bione *et al*., 1996). Clinical presentation of the disease is variable, but symptoms include cardiomyopathy, extreme fatigue, skeletal myopathy, neutropenia, and early diminished growth, along with biochemical abnormalities such as low plasma cholesterol and 3-methylglutaconic aciduria (Barth *et al*., 1999, 2004; Spencer *et al*., 2006). Based on sequence homology, TAZ has been characterized as an acyltransferase (Neuwald, 1997). Subsequent work showed that it is involved in the biosynthesis of cardiolipin (CL), a unique phospholipid almost exclusively localized to the inner mitochondrial membrane (Vreken *et al*., 2000). CL is made up of a glycerol backbone with four acyl chains that in metabolically active tissues are highly unsaturated and rich in linoleic acid ($C_{18:2}$) (Schlame *et al*., 2005). To achieve the specific set of acyl chains required by a specific tissue or organism, CL must undergo additional remodeling steps (Schlame *et al*., 2000; Sparagna and Lesnefsky, 2009). Under normal conditions, CL is degraded to monolyso-CL (MLCL) and then converted back to CL by TAZ, which transfers a fatty acyl side chain to MLCL (Xu *et al*., 2006b). Fibroblasts from BTHS patients, TAZ-deficient yeast, and TAZ-disrupted *Drosophila* demonstrate an increase in MLCL, reduced levels of the mature CL, an increase in asymmetric CL, and/or the incorporation of different CL acyl side chains as a result of TAZ deficiency (Vreken *et al*.,

[1]Department of Pediatrics, University of Florida, Gainesville, FL 32610.
[2]Powell Gene Therapy Center, University of Florida, Gainesville, FL 32610.
[3]Barth Syndrome Foundation, Perry, FL 32348.
[4]Department of Anesthesiology, New York University School of Medicine, New York, NY 10016.
[5]Department of Molecular Genetics and Microbiology, University of Florida, Gainesville, FL 32610.

2000; Gu *et al*., 2004; Malhotra *et al*., 2009). Furthermore, BTHS cells and other model systems exhibit abnormal mitochondrial cristae that appear as disorganized stacks or swirls.

Although BTHS cell lines, yeast, *Drosophila*, and zebrafish models have been useful in elucidating the molecular mechanisms involved as a consequence of TAZ deficiency, these models fall short at correlating these mechanisms with physiological abnormalities observed in cardiac and skeletal muscle (Barth *et al*., 1996; Gu *et al*., 2004; Khuchua *et al*., 2006; Xu *et al*., 2006a). Here we describe an inducible short hairpin RNA (shRNA)-mediated TAZ knockdown (TAZKD) mouse model. Traditional approaches to targeted disruption of the *TAZ* locus in the mouse have been met with difficulty by several laboratories, which led us to evaluate the utility of partial knockdown of TAZ function via RNA interference. This mouse model may provide a means to study how TAZ deficiency affects tetralinoleoyl-CL, the same predominant species found in human tissue, and how these deficiencies impact morphology and function of cardiac and skeletal muscle.

Materials and Methods

Genotyping and shRNA induction

Animals were genotyped using polymerase chain reaction (PCR) with the primers 5′ CCATGGAATTCGAACGCT GACGTC 3′ and 3′ TATGGGCTATGAACTAATGACCC 5′ for confirmation of the *TAZ* shRNA transgene, yielding a 381-bp product. Females were started on doxycycline (200 mg/kg) chow prior to fertilization and kept on the chow while nursing. Upon weaning, the pups were given doxycycline chow and remained on medicated chow for the remainder of the life span.

Real-time PCR

Total RNA was isolated using TRIzol reagent (Invitrogen, Carlsbad, CA) according to the manufacturer's protocol. Contaminating DNA was removed using DNAfree (Ambion, Austin, TX). Quantitative real-time (RT)-PCR was performed on an Applied Biosystems (Foster City, CA) Fast7300 Real-Time PCR System using Sybr Green and both TAZ- and β-actin-specific primers designed using Clone Manager software. Primer sequences were as follows: TAZ sense, 5′ AACTCCGCCACATCTGGAAC 3′; TAZ antisense, 5′ AGCG CAGGAACTCAGAACTC 3′.

Lipid analysis

Crude mitochondria were isolated from cardiac tissue, and lipids were extracted (Bligh and Dyer, 1959). Aliquots of the lipid extracts, corresponding to 0.5 mg of mitochondrial protein, were dried and redissolved in 50 μl of chloroform/methanol (1:1, v/v). Mass spectrometry was performed according to the procedure of Sun *et al*. (2008) with minor modifications. Aliquots of the extracts were diluted 1:10 in 2-propanol/acetonitrile (3:2, v/v) in order to perform matrix-assisted laser desorption/ionization (MALDI)–time of flight mass spectrometry, using 9-aminoacridine as the matrix. Spectra were recorded in negative ion mode with a MALDI micro MX mass spectrometer from Waters Chromatography (Milford, MA). The instrument was operated in reflectron mode, the pulse voltage was set to 2,000 V, and the detector voltage was set to 2,400 V. Spectra were obtained by averaging 1,000 laser shots (10 shots per subspectrum, 100 subspectra).

Electron microscopy

Freshly excised tissue samples were fixed in 2% paraformaldehyde/3% glutaraldehyde in 0.1 *M* sodium cacodylate buffer (pH 7.4) at room temperature. Subsequent procedures included postfixation with osmium tetroxide, dehydration through a graded series of alcohol solutions, treatment with propylene oxide, and embedding in epoxy resin. Semithin sections (1 μm) were mounted on glass slides, stained with toluidine blue, and observed under a light microscope to determine their anatomic orientation of muscles within the block. Thin sections (90 nm) were collected on carbon-coated grids, contrasted with uranyl acetate and lead citrate, and observed in a transmission electron microscope. Embedding and sectioning were performed by the Electron Microscopy Core Laboratory at the University of Florida College of Medicine.

Force-frequency measurements

The soleus was isolated with the tendons attached and suspended vertically in a water-jacketed tissue bath (Radnoti, Monrovia, CA) containing Krebs–Henseleit solution equilibrated with a 95% O_2/5% CO_2 gas mixture, maintained at 37°C and pH 7.4, and equilibrated for 20 min. Single-twitch contractions were evoked, followed by stepwise increases in muscle length, until maximal isometric twitch tension was obtained. All contractile properties were measured isometrically at optimum length. Peak isometric tetanic force was measured at 15, 30, 60, 100, and 160 Hz. Single 500-msec trains were used, with a 2-min recovery period. Load was measured, and the muscle was dissected away from the tendons, blotted dry, and weighed.

Magnetic resonance imaging analysis

Cardiac magnetic resonance imaging was performed on a 4.7-T Varian (Palo Alto, CA) instrument at the University of Florida Advanced Magnetic Resonance Imaging and Spectroscopy Facility. The animals were anesthetized using 1.5% isoflurane (Abbott Laboratories, North Chicago, IL) and oxygen at a flow rate of 1 L/min. The animals were placed prone on a home-built quadrature transmit-and-receive surface coil. The heart was placed as near the center of the coil as possible. Images were acquired using cardiac prospective gating triggered at the peak of the R-R wave. The heart was visualized by acquiring single short-axis slices along the length of the left ventricle, and images were processed using NIH software (ImageJ). Contours were drawn for the epicardium and the endocardium for each slice at both end diastole and end systole for each cardiac slice to determine ejection fraction and cardiac mass.

Electrocardiography

Mice were anesthetized with a mixture of 1.5–2% isoflurane and oxygen at a flow rate of 1 L/min and then positioned supine on a heating pad. Electrocardiography leads were placed subcutaneously in the right shoulder, right forelimb, left forelimb, left hindlimb, and the tail. Electro-

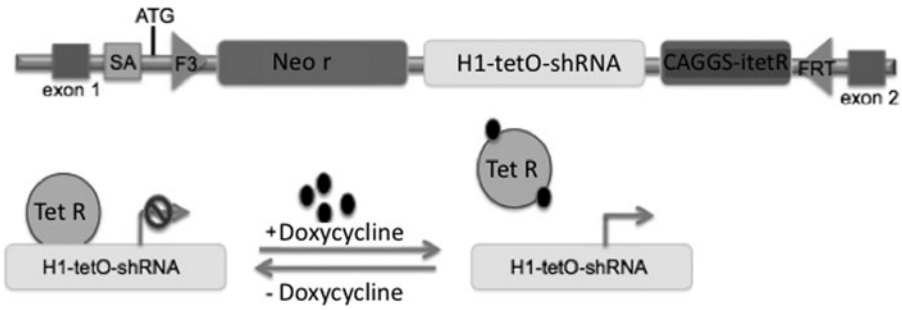

FIG. 1. Representation of the shRNA-mediated TAZKD cassette. The F3/FRT cassette was pre-engineered in the *ROSA26* locus of mouse ES cells. The cassette contains a neomycin resistance gene (*Neo r*), an H1 promoter of the tetracycline-operator (tetO) driving expression of a mouse TAZ-specific shRNA, and a tetracycline repressor (Tet R) open reading frame. Expression of the TAZ shRNA was induced upon the feeding of tetracycline to mice (200 mg/kg of chow). SA, splice acceptor.

cardiography tracings were acquired for 1 min per animal using a PowerLab AD Instruments unit and Chart acquisition software (ADInstruments, Colorado Springs, CO). Peak intervals from all tracings were averaged for each animal and then averaged within each experimental group.

Results

Generation of TAZKD mutant mice

An inducible TAZ-specific shRNA-mediated knockdown murine model was generated by TaconicArtemis GmbH (Cologne, Germany) using proprietary technology and under contract with the Barth Syndrome Foundation. The F3/FRT cassette acceptor site was pre-engineered into the *ROSA26* locus of mouse embryonic stem (ES) cells. The F3/FRT cassette consists of the H1 promoter with a tetracycline-operator controlling expression of a TAZ-specific shRNA along with a neomycin-selection gene without a promoter (Fig. 1). The cassette was then inserted into ES cells by recombinase-mediated cassette exchange, subjected to Genticin (neomycin) selection, and screened for proper insertion using Southern blots. Upon feeding doxycycline either to these correctly targeted ES cells or to mice generated from them, the shRNA is expressed, leading to the degradation of the TAZ mRNA through the RNA interference pathway. Correctly targeted mouse ES cells were analyzed by RT-PCR to confirm TAZ mRNA knockdown. Several shRNA sequences were designed and tested. One construct resulted in significant knockdown (65%) by targeting the splice junction between murine exons 6 and 7 (homologous to human exons 7 and 8, as the murine *TAZ* gene does not contain an exon homologous to the human exon 5) (Lu *et al.*, 2004). CL lowering and MLCL accumulation were confirmed in these ES cells by high-performance liquid chromatography–mass spectroscopy analysis. Germline transmission was confirmed in the resultant mice, and two breeder pairs were transferred to the University of Florida for characterization.

Induction of TAZ shRNA leads to a reduction in TAZ mRNA levels in vivo

In order to induce shRNA expression *in vivo*, breeding pairs were fed doxycycline chow, and pups were maintained on medicated chow for the remainder of the experiments. At 2 months of age, quantitative RT-PCR was performed using RNA extracted from heart, tibialis anterior, liver, and brain tissue. Induction of shRNA led to a significant reduction in TAZ mRNA levels in all tissues tested at 2 months ($89.9 \pm 1.5\%$ in heart, $94.7 \pm 0.3\%$ in tibialis anterior, $71.0 \pm 8.6\%$ in liver, and $82.2 \pm 7.5\%$ in brain) compared with transgenic littermates not on doxycycline (Fig. 2) ($p < 0.05$ for all tissues). We attempted to confirm that the RNA knockdown was paralleled by a loss in TAZ protein, but the commercial antibodies that were available against TAZ reacted with many proteins that it was difficult to predict which, if any, corresponded to TAZ.

TAZKD results in impaired CL remodeling

TAZKD in cardiac tissue led to an alteration in the CL profile and an increase in the MLCL/CL ratio at 2 months of age. MALDI–time of flight analysis revealed the presence of a more saturated CL species (68:2-CL [$m/z = 1{,}404$], 70:3-CL [$m/z = 1{,}430$]) along with the absence of tetralinoleoyl-CL (72:8) in TAZKD cardiac samples. In addition to a reduction in total CL, TAZKD showed a significant accumulation of MLCL species (52:2-MLCL [$m/z = 1{,}166$], 54:4-MLCL [$m/z = 1{,}190$], and 54:3-MLCL [$m/z = 1{,}192$]), which was not seen in control littermates (Fig. 3).

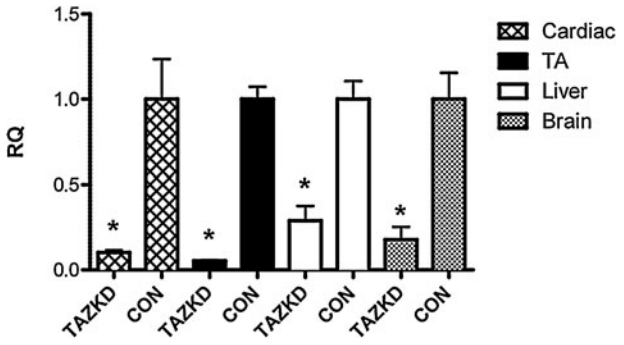

FIG. 2. shRNA-mediated TAZKD in TAZKD animals. RT-PCR analysis 2 months after shRNA induction showed reduced Taz mRNA by $89.9 \pm 1.5\%$ in cardiac, $94.7 \pm 0.3\%$ in tibialis anterior (TA), $71.0 \pm 8.6\%$ in liver, and $82.2 \pm 7.5\%$ in brain tissues. Data are mean $\pm$ SEM values. $^*p \leq 0.05$. β-Actin was used as an endogenous control. RQ, relative quantity, CON, control non-induced transgenic mice; TAZKD, doxycycline-induced transgenic mice.

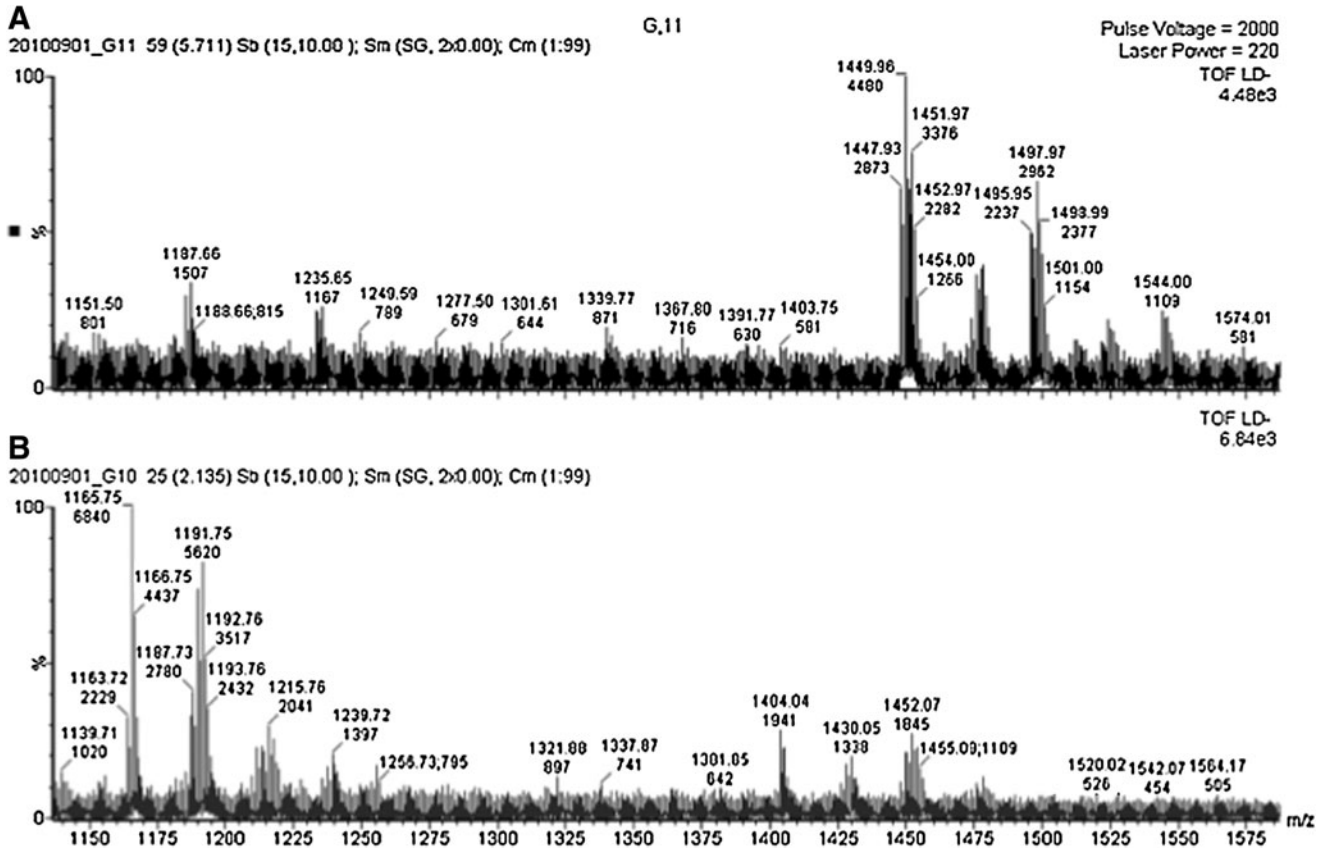

FIG. 3. CL analysis of cardiac tissue in TAZKD animals: **(A)** typical CL profile in control animals and **(B)** reduction in tetralineoyl-CL with a concomitant increase in MLCL moieties in TAZKD animals. CON, control doxycycline-treated non-transgenic mice; TAZKD, doxycycline-induced transgenic mice; TOF, time of flight.

Knockdown of TAZ causes mitochondrial abnormalities

To investigate the effects of TAZKD on mitochondrial structure we performed electron microscopy of both cardiac and skeletal muscle. Previous studies have shown that mitochondria from both BTHS patients and TAZ-deficient models show signs of ultrastructural abnormalities—specifically, disorganized cristae that appear as hyperdense stacks or swirls and/or giant mitochondria (Barth *et al.*, 1996; Gu *et al.*, 2004; Xu *et al.*, 2006a). We did not observe abnormal ultrastructural morphology of cristae in cardiac mitochondria at 2 months, but we noticed that TAZKD tissue contain swollen mitochondria resulting in a decrease in cardiac myofiber density compared with controls (Fig. 4). However, remaining cardiac myofibers did not display morphological alterations. Examination of soleus muscle revealed abnormal mitochondria dispersed among normal mitochondria in TAZKD samples. Abnormal mitochondria showed a disruption of the cristae, presenting as electron-dense structures within the inner mitochondrial membrane. Upon further magnification, these cristae formed whorls lining the inner membrane wall (Fig. 4).

Skeletal muscle contractile properties are impaired in TAZKD mice

To determine whether TAZKD mice exhibit skeletal muscle dysfunction, *ex vivo* isometric force-frequency measurements were performed on soleus muscle from TAZKD and control mice. Force-frequency measurements revealed a significant decrease in force generated when stimulated at $\geq$100 Hz at 2 months ($n = 3$ for each group): 100 Hz, control 14.85 ± 0.82 N/cm^2, TAZKD 11.84 ± 1.05 N/cm^2; 160 Hz, control 15.91 ± 0.91 N/cm^2, TAZKD 11.87 ± 1.10 N/cm^2 (Fig. 5, $p<0.05$).

Cardiac dysfunction is evident in TAZKD mice

Cardiac function for left ventricular ejection fraction and left ventricular diastolic mass of experimental and control groups was evaluated at 7 and 10 months of age. Magnetic resonance imaging analysis demonstrated an approximate 20% decrease in ejection fraction at both 7 (TAZKD, $45.38 \pm 3.21\%$; control, $66.62 \pm 2.37\%$) and 10 (TAZKD, $45.40 \pm 6.06\%$; control, $66.83 \pm 1.20\%$) months of age in TAZKD mice compared with age-matched controls (Fig. 6, $p < 0.05$). Left ventricular diastolic mass was unchanged at both 7 (TAZKD, 7.53 ± 0.61; control, 7.56 ± 0.37) and 10 (TAZKD, 6.00 ± 0.35; control, 5.52 ± 0.16) months (data not shown) when left ventricular mass was normalized to body mass ($n = 4$ for each group and age point). Electrocardiographic analysis at 3, 6, and 9 months of age did not reveal any abnormalities in heart rate or electrical activity (data not shown).

Discussion

BTHS patient cell lines, yeast, *Drosophila*, and zebrafish models have been important in the biochemical character-

ization of TAZ deficiency on CL remodeling and on mitochondrial function (Vaz *et al.*, 2003; Khuchua *et al.*, 2006; Xu *et al.*, 2006a), but none of these model systems permits study of the effects of mutations in the *TAZ* gene on the mammalian heart or in an *in vivo* system where tetralinoleoyl-CL is the dominant CL species. Our study introduces the first mammalian model of BTHS, which will be utilized to evaluate the pathogenesis and potential treatments for the disease. We have characterized an inducible shRNA-mediated TAZKD mouse model and report alteration of CL profiles, abnormal mitochondrial morphology, skeletal muscle weakness, and cardiomyopathy. The model has been made available to all investigators with an interest in CL, in mitochondrial bioenergetics, or specifically in BTHS, and we anticipate data supportive of these findings will be forthcoming.

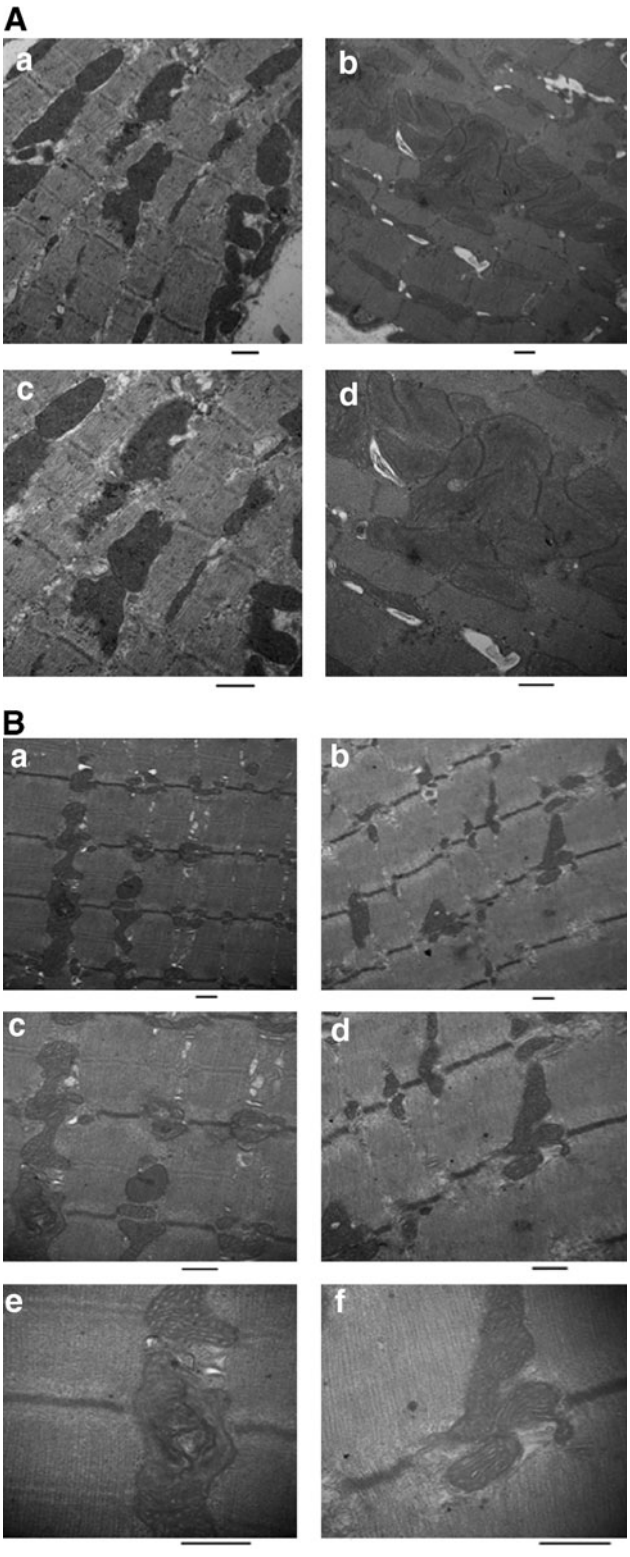

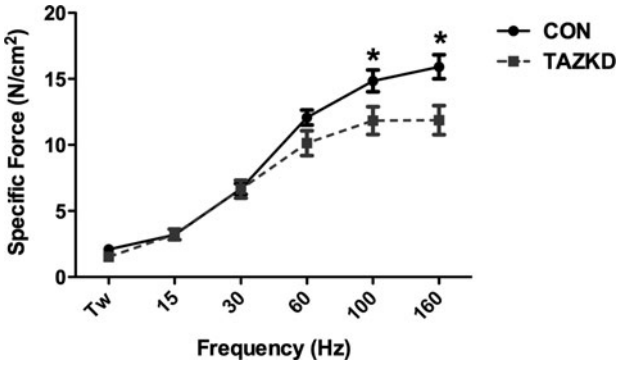

FIG. 5. Force-frequency characteristics of soleus muscle in TAZKD animals. At 2 months of age soleus muscle from TAZKD animals exhibited a significant reduction in force generation when stimulated at frequencies of $\geq$100 Hz compared with controls. Data are mean $\pm$ SEM values ($n = 6$). *$p \leq 0.05$. TW, twitch; CON, control doxycycline non-transgenic mice; TAZKD, doxycycline-induced transgenic mice.

TAZ deficiency results in an inability to form normal amounts of tetralinoleoyl CL, resulting in a more saturated CL species and an accumulation of the CL degradation product, MLCL (Vreken *et al.*, 2000; Valianpour *et al.*, 2005). Mitochondria from BTHS patient cells, TAZ-deficient yeast, and TAZ-disrupted *Drosophila* demonstrate abnormal swirls and stacks of cristae in the inner mitochondrial membrane. These features are believed to be a direct effect of alterations in the predominant CL species profile based on data obtained from the evaluation of BTHS patient cell lines and *Drosophila* wing muscle mitochondria (Xu *et al.*, 2006a). Although the predominant tetralinoleoyl-CL species is absent in TAZKD cardiac tissue, abnormalities in mitochondrial cristae in cardiac mitochondria were not detected at 2 months of age. This result indicates that mitochondria are able to maintain inner membrane integrity although the

FIG. 4. Ultrastructural characteristics of cardiac and soleus muscle in TAZKD animals at 2 months of age. **(A)** Electron microscopy of thin sections of TAZKD hearts reveals the appearance of giant mitochondria accumulating between myofibers **(b** and **d)** compared with controls **(a** and **c)**. **(B)** Electron microscopy of TAZKD soleus muscle reveals electron-dense stacks in the inner membrane along with tubular and swirled cristae in TAZKD mice **(a**, **c**, and **e)** compared with controls **(b**, **d**, and **f)**. Original magnifications: **(A** and **B) (a** and **b)** $\times$15,000, **(c** and **d)** $\times$25,000; **(B) (e** and **f)** $\times$50,000. CON, control doxycycline non-transgenic mice; TAZKD, doxycycline-induced transgenic mice. Scale bar = 500 nm.

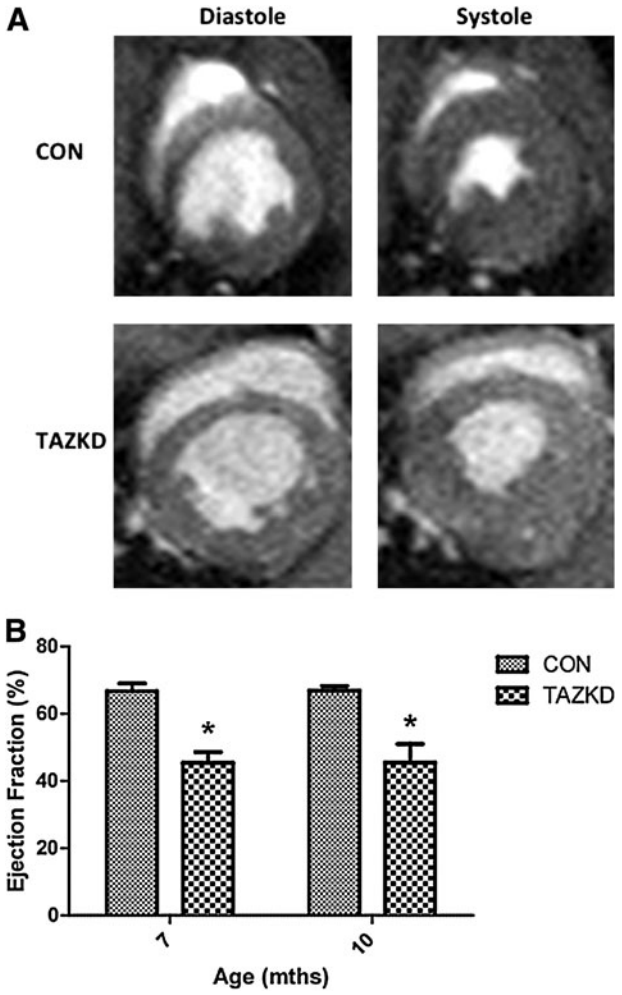

FIG. 6. Cardiac function in TAZKD animals at 7 and 10 months of age. **(A)** Representation of the left ventricle during diastole and systole at 10 months. **(B)** Ejection fraction in TAZKD animals was significantly reduced at 7 and 10 months of age. Data are mean ± SEM values ($n = 4$). *$p \leq 0.05$. CON, control non-induced transgenic mice; TAZKD, doxycycline-induced transgenic mice.

normal CL species is absent. We hypothesize that maintenance of normal structure may be possible only while the mice are sedentary and that cristae abnormalities will become apparent upon increasing the metabolic demand in the mice. In a spontaneous hypertensive heart failure rat model, an increase in metabolic stress results in an acceleration of mitochondrial rearrangements, cardiac myopathy, and mitochondrial dysfunction (Reibel *et al.*, 1986; Dhalla *et al.*, 1993).

Cardiac and skeletal myopathies have been reported as common physiological consequences of TAZ deficiency (Barth *et al.*, 2004; Spencer *et al.*, 2006). The mouse model described here is the first model to allow for examination of the physiological effects of TAZ deficiency. There was no apparent difference in locomotor activity of TAZKD and control mice; however, we determined that TAZKD mice had a significant reduction in cardiac and skeletal muscle function. The reduction in soleus contractile strength and decrease in left ventricular ejection force may be due to, but not limited to, mitochondrial insufficiency, loss of calcium homeostasis, oxidative stress, or disruption of contractile components (*i.e.*, increase in proteolytic mechanisms). Further assessment of these potential mechanisms may reveal the processes in which cardioskeletal muscle dysfunction occurs in this model.

Neutropenia is a variable feature of the disease, which has remained poorly understood throughout the investigation and characterization of BTHS. A clinical study by Spencer *et al*. (2006) demonstrated that 25% of patients had abnormal neutrophil levels. We investigated neutrophil levels in 2-month-old mice and found that 50% of TAZKD mice had low neutrophil counts as well as 20% of control mice (data not shown). We believe that these data are complicated by the doxycycline diet that is necessary to induce shRNA expression in mice. Doxycycline (part of the tetracycline family) has been reported to reduce neutrophil counts; therefore, this doxycycline-inducible tetracycline-on system may hamper further investigation of neutropenia in this model (Abdul-Hussien *et al.*, 2009).

The TAZ-deficient mouse model effectively mimics some of the major molecular and physiological characteristics observed in BTHS patients and should be helpful for further investigation of BTHS pathogenesis. Future experiments will examine potential treatment modalities to mitigate cardiovascular, skeletal muscle, and immune deficits seen in this disease, particularly the opportunity to replace TAZ function by gene transfer.

Acknowledgments

The authors gratefully acknowledge the following groups: The University of Florida Advanced Magnetic Resonance Imaging and Spectroscopy Facility for development and assistance with cardiac magnetic resonance imaging measurements, The University of Florida Electron Microscopy Core for embedding and sectioning of electron microscopy samples, and the Barth Syndrome Foundation for providing the tafazzin knockdown mice. This article is dedicated to the memory of Michael Bowen Jr. and Ben Thorpe, whose courage and leadership have been an inspiration to many fellow patients and the entire Barth community. This work was supported by grants 15T32HL083810-04 (to M.S.S.) and 5F32HL095282-03 (to D.J.F.).

Author Disclosure Statement

No competing financial interests exist for any of the authors. M.J.T. is Science Director of the Barth Syndrome Foundation, and B.J.B. is a member of the Barth Syndrome Foundation Scientific Advisory Board.

References

Abdul-Hussien, H., Hanemaaijer, R., Verheijin, J.H., *et al*. (2009). Doxycycline therapy for abdominal aneurysm: Improved proteolytic balance through reduced neutrophil content. J. Vasc. Surg. 49, 741–749.

Barth, P.G., Scholte, H.R., Berden, J.A., *et al*. (1983). An X-linked mitochondrial disease affecting cardiac muscle, skeletal muscle and neutrophil leucocytes. J. Neurol. Sci. 62, 327–355.

Barth, P.G., van den Bogert, C., Bolhuis, P.A., *et al*. (1996). X-linked cardioskeletal myopathy and neutropenia (Barth

syndrome): Respiratory-chain abnormalities in cultured fibroblasts. J. Inherit. Metab. Dis. 19, 157–160.
Barth, P.G., Wanders, R.J., Vreken, P., *et al*. (1999). X-linked cardioskeletal myopathy and neutropenia (Barth syndrome) (MIM 302060). J. Inherit. Metab. Dis. 22, 555–567.
Barth, P.G., Valianpour, F., Bowen, V.M., *et al*. (2004). X-linked cardioskeletal myopathy and neutropenia (Barth syndrome): An update. Am. J. Med. Genet. A 126A, 349–354.
Bione, S., D'Adamo, P., Maestrini, E., *et al*. (1996). A novel X-linked gene, G4.5, is responsible for Barth syndrome. Nat. Genet. 12, 385–389.
Bligh, E.G., and Dyer, W.J. (1959). A rapid method of total lipid extraction and purification. Can. J. Biochem. Physiol. 37, 911–917.
Bolhuis, P.A., Hensels, G.W., Hulsebos, T.J., *et al*. (1991). Mapping of the locus for X-linked cardioskeletal myopathy with neutropenia and abnormal mitochondria (Barth syndrome) to Xq28. Am. J. Hum. Genet. 48, 481–485.
Dhalla, N.S., Afzal, N., Beamish, R.E., *et al*. (1993). Pathophysiology of cardiac dysfunction in congestive heart failure. Can. J. Cardiol. 9, 873–887.
Gu, Z., Valianpour, F., Chen, S., *et al*. (2004). Aberrant cardiolipin metabolism in the yeast taz1 mutant: A model for Barth syndrome. Mol. Microbiol. 51, 149–158.
Khuchua, Z., Yue, Z., Batts, L., and Strauss, A.W. (2006). A zebrafish model of human Barth syndrome reveals the essential role of tafazzin in cardiac development and function. Circ. Res. 99, 201–208.
Lu, B., Kelher, M.R., Lee, D.P., *et al*. (2004). Complex expression pattern of the Barth syndrome gene product tafazzin in human cell lines and murine tissues. Biochem. Cell Biol. 82, 569–576.
Malhotra, A., Edelman-Novemsky, I., Xu, Y., *et al*. (2009). Role of calcium-independent phospholipase A2 in the pathogenesis of Barth syndrome. Proc. Natl. Acad. Sci. U.S.A. 106, 2337–2341.
Neuwald, A.F. (1997). Barth syndrome may be due to an acyltransferase deficiency. Curr. Biol. 7, R465–R466.
Reibel, D.K., O'Rourke, B., Foster, K.A., *et al*. (1986). Altered phospholipid metabolism in pressure-overload hypertrophied hearts. Am. J. Physiol. 250, H1–H6.
Schlame, M., Rua, D., and Greenberg, M.L. (2000). The biosynthesis and functional role of cardiolipin. Prog. Lipid Res. 39, 257–288.
Schlame, M., Ren, M., Xu, Y., *et al*. (2005). Molecular symmetry in mitochondrial cardiolipins. Chem. Phys. Lipids 138, 38–49.
Sparagna, G.C., and Lesnefsky, E.J. (2009). Cardiolipin remodeling in the heart. J. Cardiovasc. Pharmacol. 53, 290–301.
Spencer, C.T., Bryant, R.M., Day, J., *et al*. (2006). Cardiac and clinical phenotype in Barth syndrome. Pediatrics 118, e337–e346.
Sun, G., Yang, K., Zhao, Z., *et al*. (2008). Matrix-assisted laser desorption/ionization time-of-flight mass spectrometric analysis of cellular glycerophospholipids enabled by multiplexed solvent dependent analyte-matrix interactions. Anal. Chem. 80, 7576–7585.
Valianpour, F., Mitsakos, V., Schlemmer, D., *et al*. (2005). Monolysocardiolipins accumulate in Barth syndrome but do not lead to enhanced apoptosis. J. Lipid Res. 46, 1182–1195.
Vaz, F.M., Houtkooper, R.H., Valianpour, F., *et al*. (2003). Only one splice variant of the human TAZ gene encodes a functional protein with a role in cardiolipin metabolism. J. Biol. Chem. 278, 43089–43094.
Vreken, P., Valainpour, F., Nijtmans, L.G., *et al*. (2000). Defective remodeling of cardiolipin and phosphatidylglycerol in Barth syndrome. Biochem. Biophys. Res. Commun. 279, 378–382.
Xu, Y., Condell, M., Plesken, H., *et al*. (2006a). A *Drosophila* model of Barth syndrome. Proc. Natl. Acad. Sci. U.S.A. 103, 11584–11588.
Xu, Y., Malhotra, A., Ren, M., and Schlame, M. (2006b). The enzymatic function of tafazzin. J. Biol. Chem. 281, 39217–39224.

Address correspondence to:
Dr. Barry J. Byrne
Department of Pediatrics
University of Florida College of Medicine
P.O. Box 103610
Gainesville, FL 32610

E-mail: bbyrne@ufl.edu

Received for publication October 8, 2010;
accepted after revision December 12, 2010.

Published online: December 13, 2010.